A Priori Subgrid Scale Modeling for a Droplet Laden Temporal Mixing Layer

Nora Okong'o and Josette Bellan
Jet Propulsion Laboratory
California Institute of Technology
Pasadena CA 91109-8099

Abstract

Subgrid analysis of a transitional temporal mixing layer with evaporating droplets has been performed using a direct numerical simulation (DNS) database. The DNS is for a Reynolds number (based on initial vorticity thickness) of 600, with droplet mass loading of 0.2. The gas phase is computed using a Eulerian formulation, with Lagrangian droplet tracking. Since Large Eddy Simulation (LES) of this flow requires the computation of unfiltered gas-phase variables at droplet locations from filtered gas-phase variables at the grid points, it is proposed to model these by assuming the gas-phase variables to be given by the filtered variables plus a correction based on the filtered standard deviation, which can be computed from the subgrid scale (SGS) standard deviation. This model predicts the unfiltered variables at droplet locations better than simply interpolating the filtered variables. Three methods are investigated for modeling the SGS standard deviation: Smagorinsky, gradient and scale-similarity. When properly calibrated, the gradient and scale-similarity methods give results in excellent agreement with the DNS.

Introduction

Droplet-laden turbulent flows occur in many problems of practical interest, such as spray combustion and atomization. The interaction of particles and turbulence is an integral feature of such flows, and hence the topic of much research [2][3][5][12]. Large Eddy Simulation (LES), in which the flow field is spatially filtered, is emerging as a powerful tool in modelling unsteady turbulent flows. It is expected to be more generally applicable than Reynolds-Averaged Navier Stokes (RANS), since the large scale structures are computed, and the more universal small scale structures are modelled. LES is also less computationally intensive than direct numerical simulation (DNS) in which all length scales are resolved, and has the additional advantage of being able to accommodate considerably larger Reynolds numbers (Re). Whereas much research has been devoted to LES modeling for single phase incompressible flows, only moderate attention has been given to compressible shear flows [1][15], with focus now turning two-phase flows [4][11][16]. In addition to modeling subgrid scale (SGS) terms for the gas phase, an LES of a droplet-laden flow would require modeling the unfiltered gas phase variables at the droplet locations. In simplistic models, the filtered variables are substituted for the unfiltered variables; however, this assumption may be substantially inaccurate for droplets with small Stokes numbers. With an increasing body of DNS computations [5][6][7][8][13][14], it is now possible to assess subgrid scale quantities at moderate Reynolds numbers, with good prospects for devising subgrid scale models.

Recently, Miller and Bellan [9][10] have performed DNS of droplet laden mixing layers. They use 'DNS' to refer to computations in which all length scales of the gas-phase are resolved but the effect of the gas on each droplet is modeled using Stokes drag, and the effect of the droplets on the gas are modeled as source terms in the gas-phase equations. The present paper addresses the use of the DNS database of Miller and Bellan [9] to evaluate subgrid scale closures. Specifically, we examine the largest Reynolds number (based on initial vorticity thickness, $\delta_{\omega,0}$, and initial velocity difference, ΔU_0) of 600, with mass loading of 0.2 (3×10^6drops) on a $300\times332\times180$ ($0.25\text{m}\times0.22\text{m}\times0.12\text{m}$) grid, which they denote as case TP600.

Governing Equations

The governing equations for the gas phase density (ρ), velocity (u_i), total energy (E) and vapor mass fraction (Y_V) are given by:

$$\frac{\partial \rho}{\partial t} + \frac{\partial}{\partial x_j}\left[\rho u_j\right] = S_I \tag{1}$$

$$\frac{\partial \rho u_i}{\partial t} + \frac{\partial}{\partial x_j}\left[\rho u_i u_j + P\delta_{ij} - \sigma_{ij}\right] = S_{II,i} \tag{2}$$

$$\frac{\partial \rho E}{\partial t} + \frac{\partial}{\partial x_j}\left[\left(\rho E + P\right)u_j - \lambda\frac{\partial T}{\partial x_j} - u_i\sigma_{ij}\right] = S_{III} \tag{3}$$

$$\frac{\partial \rho Y_V}{\partial t} + \frac{\partial}{\partial x_j}\left[\rho Y_V u_j - \rho\Gamma\frac{\partial Y_V}{\partial x_j}\right] = S_I \tag{4}$$

$$\sigma_{ij} = \mu\left(\frac{\partial u_i}{dx_j} + \frac{\partial u_j}{dx_i} - \frac{2}{3}\frac{\partial u_k}{dx_k}\delta_{ij}\right) \tag{5}$$

$$P = \rho R T \tag{6}$$

$$E = \tfrac{1}{2}u_i u_i + C_v T + h_V^0 Y_V \tag{7}$$

$$R = Y_V R_V + \left(1 - Y_V\right)R_C \tag{8}$$

$$C_v = Y_V C_{v,V} + \left(1 - Y_V\right)C_{v,C} \tag{9}$$

where subscript V denotes the vapor, subscript C denotes the carrier gas, and the mass fraction of the carrier gas is $Y_C = 1 - Y_V$.

The Lagrangian particle equations for the position (X_i), velocity (v_i) temperature (T_d) and mass (m_d) are:

$$\frac{dX_i}{dt} = v_i \tag{10}$$

$$\frac{dv_i}{dt} = \frac{F_i}{m_d} \tag{11}$$

$$\frac{dT_d}{dt} = \frac{Q + \frac{dm_d}{dt} L_v}{m_d C_L} \tag{12}$$

Computation of the drag force F_i, the heat flux Q and the evaporation rate $\frac{dm_d}{dt}$ require knowledge of the gas phase variables (u_i, T, Y_V, P) at the droplet locations, and involve validated relations [10].

The source terms are

$$S_I = -\sum \left[\tfrac{dm_d}{dt}\right] \tag{13}$$

$$S_{II,i} = -\sum \left[F_i + \tfrac{dm_d}{dt} v_i\right] \tag{14}$$

$$S_{III} = -\sum \left[F_i v_i + Q + \tfrac{dm_d}{dt}\left(\tfrac{1}{2} v_i v_i + C_{p,V} T_d + h_V^0\right)\right] \tag{15}$$

where $\sum$ indicates appropriately weighted summations over droplets within a discretization volume associated with each grid point.

Filtered Governing Equations

The filtering operation is defined as:

$$\overline{\phi}(\overrightarrow{x}) = \int_V \phi(\overrightarrow{y}) G(\overrightarrow{x} - \overrightarrow{y}) d\overrightarrow{y} \tag{16}$$

where G is the filter function, with the property that $\overline{1} = 1$, and V is the filtering volume. We use a cubic top-hat filter, in which V is a cube of sides Δ, and G is simply a volume-average. For compressible flow, we use Favre filtering, defined as $\widetilde{\phi} = \overline{\rho\phi}/\overline{\rho}$, to simplify the notation. After filtering, the gas phase equations become:

$$\frac{\partial \overline{\rho}}{\partial t} + \frac{\partial}{\partial x_j}\left[\overline{\rho}\widetilde{u}_j\right] = \overline{S}_I \tag{17}$$

$$\frac{\partial \overline{\rho}\widetilde{u}_i}{\partial t} + \frac{\partial}{\partial x_j}\left[\overline{\rho}\widetilde{u}_i\widetilde{u}_j + \overline{P}\delta_{ij} - \widetilde{\sigma}_{ij} + \overline{\rho}\tau_{ij}\right] = \overline{S}_{II,i} \tag{18}$$

$$\frac{\partial \overline{\rho}\widetilde{E}}{\partial t} + \frac{\partial}{\partial x_j}\left[\left(\overline{\rho}\widetilde{E} + \overline{P}\right)\widetilde{u}_j - \lambda\frac{\partial \overline{T}}{\partial x_j} - \widetilde{u}_i\widetilde{\sigma}_{ij}\right] + \frac{\partial}{\partial x_j}\left[\widetilde{u}_i\overline{\rho}\tau_{ij} + \widetilde{C}_p\overline{\rho}\theta_j + h_V^0\overline{\rho}\eta_j\right] = \overline{S}_{III} \tag{19}$$

$$\frac{\partial \overline{\rho}\widetilde{Y}_V}{\partial t} + \frac{\partial}{\partial x_j}\left[\overline{\rho}\widetilde{Y}_V\widetilde{u}_j - \overline{\rho}\Gamma\frac{\partial \widetilde{Y}_V}{\partial x_j} + \overline{\rho}\eta_j\right] = \overline{S}_I \tag{20}$$

where

$$\tau_{ij} = \widetilde{u_i u_j} - \widetilde{u}_i\widetilde{u}_j \tag{21}$$

$$\theta_j = \widetilde{Tu_j} - \overline{T}\widetilde{u}_j \tag{22}$$

$$\eta_j = \widetilde{Y_V u_j} - \widetilde{Y}_V\widetilde{u}_j \tag{23}$$

$$\widetilde{\sigma}_{ij} = \mu\left(\frac{\partial \widetilde{u}_i}{dx_j} + \frac{\partial \widetilde{u}_j}{dx_i} - \frac{2}{3}\frac{\partial \widetilde{u}_k}{dx_k}\delta_{ij}\right) \tag{24}$$

$$\widetilde{C}_p = \widetilde{Y}_V C_{p,V} + (1 - \widetilde{Y}_V) C_{p,C} \tag{25}$$

$$\widetilde{C}_v = \widetilde{Y}_V C_{v,V} + \left(1 - \widetilde{Y}_V\right) C_{v,C} \tag{26}$$

$$\widetilde{R} = \widetilde{Y}_V R_V + \left(1 - \widetilde{Y}_V\right) R_C = \widetilde{C}_p - \widetilde{C}_v \tag{27}$$

and it has been assumed that

$$\overline{\sigma}_{ij} = \widetilde{\sigma}_{ij} \tag{28}$$

$$\tfrac{1}{2}(\overline{\rho u_i u_i u_j} - \overline{\rho u_i u_i}\widetilde{u}_j) = -\overline{\rho}\tau_{ij}\widetilde{u}_i \tag{29}$$

$$\overline{u_i\sigma_{ij}} = \widetilde{u}_i\widetilde{\sigma}_{ij} \tag{30}$$

$$\overline{\rho Y_V T} = \overline{\rho Y_V}\,\overline{T} \tag{31}$$

$$\overline{\rho Y_V T u_j} - \overline{\rho Y_V T}\widetilde{u}_j = \overline{\rho Y_V}\left(\widetilde{Tu_j} - \overline{T}\widetilde{u}_j\right) \tag{32}$$

$$\overline{P} = \overline{\rho}\widetilde{R}\overline{T} \tag{33}$$

$$\widetilde{E} = \tfrac{1}{2}\widetilde{u}_i\widetilde{u}_i + \widetilde{C}_v\overline{T} + h_V^0\widetilde{Y}_V + \tfrac{1}{2}\tau_{ii} \tag{34}$$

The terms that need to be modeled are the subgrid stress τ_{ij}, the subgrid heat flux θ_j and the subgrid species flux η_j.

The droplet equations remain as before, except that now the gas-phase variables (u_i, T, Y_V, P) at the droplet locations are no longer immediately available, and will need to be derived from the filtered variables $(\widetilde{u}_i, \overline{T}, \widetilde{Y}_V, \overline{P})$. Thus the (unfiltered) gas-phase variables also need to be modeled.

Model for Instantaneous Variables

The droplet model requires modeling gas phase variables at droplet locations. To guide the modeling, we will first consider the known DNS generic variable ϕ and its filtered form $\overline{\phi}$, where the bar denotes Favre filtering for u_i and Y_V and regular filtering for T and P. The definition of the standard deviation is

$$\sigma = \sqrt{\phi\prime\phi\prime} = \sqrt{(\phi - \overline{\phi})^2} \tag{35}$$

Thus the relation between ϕ and $\overline{\phi}$ is

$$\phi = \overline{\phi} + f\sigma \tag{36}$$

where from the definition of σ, $f = \pm 1$. The goal of the modeling is to compute, from the filtered flowfield, the form of $f\sigma$ that provides a better approximation to ϕ than does $f\sigma = 0$. In this formulation, $f\sigma$ can be viewed as a correction to $\overline{\phi}$with sign f and magnitude σ.

It is tempting to assume that f randomly takes on values of -1 and 1. However, if the filtering operation is viewed as a volume average, a relation between ϕ and $\overline{\phi}$ can be derived as follows. Consider the third-order Taylor

expansion of ϕ in the filtering volume V of size Δ with centroid at $x_0 = (x_{1_0}, x_{2_0}, x_{3_0})$ integrated over the volume:

$$\overline{\phi}(x_0) = \frac{1}{V}\int_V \phi(x)dV \tag{37}$$

$$\phi(x) = \phi(x_0) + \frac{\partial\phi}{\partial x_i}(x_0)(x_i - x_{i_0})$$

$$+\frac{\partial^2\phi}{\partial x_i \partial x_j}(x_0)\tfrac{1}{2}(x_i - x_{i_0})(x_j - x_{j_0}) + O(\Delta^3) \tag{38}$$

From the definition of the centroid $\frac{1}{V}\int_V (x_i - x_{i_0})dV = 0$. If V is symmetric, then

$$\frac{1}{V}\int_V (x_i - x_{i_0})(x_j - x_{j_0})dV = 0;\ i \neq j \tag{39}$$

and

$$I_c\Delta^2 = \frac{1}{V}\int_V (x_i - x_{i_0})(x_j - x_{j_0})dV;\ i = j \tag{40}$$

is the (positive) moment of inertia, so

$$\overline{\phi} = \phi + \nabla^2\phi\frac{I_c\Delta^2}{2} + O\left(\Delta^4\right) \tag{41}$$

where terms of $O(\Delta^3)$ vanish due to the symmetry of the filtering volume.

Thus f will generally be $-sign\left(\nabla^2\phi\right)$. From the available filtered quantities, we can compute $\nabla^2\overline{\phi}$ rather than $\nabla^2\phi$; so to model f we assume that $\nabla^2\overline{\phi}$ and $\nabla^2\phi$ have the same sign. To model σ, we note that for the gas phase we will be modeling terms of the form $\overline{\phi\phi} - \overline{\phi}\,\overline{\phi}$, which are the subgrid scale fluctuations. Defining σ_{SGS} as the SGS standard deviation,

$$\sigma_{SGS} = \sqrt{\overline{\phi\phi} - \overline{\phi}\,\overline{\phi}} \tag{42}$$

The relationship between σ and σ_{SGS} can be illuminated by considering $\overline{\sigma^2}$:

$$\overline{\sigma^2} = \overline{\left(\phi - \overline{\phi}\right)^2} = \overline{\phi\phi} - 2\overline{\phi}\,\overline{\overline{\phi}} + \overline{\overline{\phi}\,\overline{\phi}} \tag{43}$$

We note that $\overline{\phi\phi} = \sigma^2_{SGS} + \overline{\phi}\,\overline{\phi}$ and that $\overline{\phi}\,\overline{\overline{\phi}}$ can be written in terms of the local correlation between ϕ and $\overline{\phi}$

$$R(\phi, \overline{\phi}) = \frac{\overline{\phi}\,\overline{\overline{\phi}}}{\sqrt{\overline{\phi\phi}}\sqrt{\overline{\overline{\phi}\,\overline{\phi}}}} \tag{44}$$

If we assume that $R(\phi, \overline{\phi}) \simeq 1$, then

$$\overline{\sigma^2} = \left(\sqrt{\overline{\phi\phi}} - \sqrt{\overline{\overline{\phi}\,\overline{\phi}}}\right)^2 = \left(\sqrt{\sigma^2_{SGS} + \overline{\phi}\,\overline{\phi}} - \sqrt{\overline{\overline{\phi}\,\overline{\phi}}}\right)^2 \tag{45}$$

Defining $\overline{\sigma} = \sqrt{\overline{\sigma^2}}$, and using $\overline{\sigma}$ as a model for σ, we arrive at a model for ϕ of the form

$$\phi = \overline{\phi} - sign(\nabla^2\overline{\phi})\overline{\sigma} \tag{46}$$

i.e. $f = -sign(\nabla^2\overline{\phi})$, $\sigma = \overline{\sigma}$. To assess this model, we will use the "exact" $\overline{\sigma}$ obtained by filtering the DNS flowfield, and then turn our attention to modeling it based on the filtered flowfield. The proposed model will be computed at the grid points, and then interpolated to the droplet locations.

Figure 1 shows the probability density function(PDF) for $(\phi - \overline{\phi})/\overline{\sigma}$ for case TP600 at the end of the simulation. These results were obtained using a cubic top-hat (box) filter with filter width $\Delta = 4\Delta x$. Notably, for all quantities there are peaks near 1, and for the velocity components there are also peaks near -1, similar to the PDF of $(\phi - \overline{\phi})/\sigma$, which takes on values of ± 1.

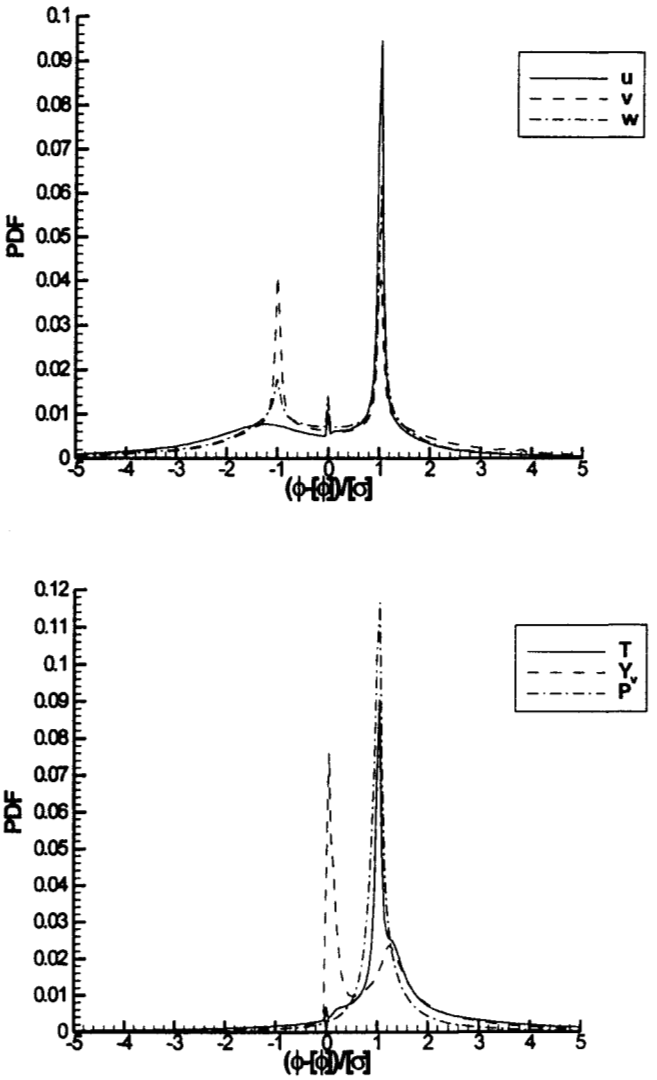

Figure 1: PDF of $(\phi - \overline{\phi})/\overline{\sigma}$

Figures 2 and 3 show the comparison between interpolating the DNS flowfield to the droplet locations (the "exact" quantities) and interpolating the models to the droplet locations. Results are presented in terms of av-

erages over droplets within a given y-interval; this averaging is denoted by $<<>>$. First, using σ as given by Equation 35, we compare the models for f. It is seen that $f = 0$ leads to significant discrepancy between the exact and model interpolated variable. Any model with f with mean 0 will not perform any better as the deviations toward the exact value will be just as likely as the deviations away from the exact values. This is seen in the case where f is randomly taken to be -1 or +1, which performs slightly worse than $f = 0$ despite having the exact σ. Using $f = -sign(\nabla^2\overline{\phi})$ gives significant improvement in view of the two assumptions made i.e. $f = -sign(\nabla^2\phi)$ and $sign(\nabla^2\phi) = sign(\nabla^2\overline{\phi})$. For the data shown in Figures 2 and 3, this is true (86%, 86%, 86%, 85%, 86% and 93%) of the time for u_1, u_2, u_3, T, Y_V, and P respectively. When σ is replaced by $\overline{\sigma}$ (denoted $[\sigma]$ in the figures), with $f = -sign(\nabla^2\overline{\phi})$, there is considerable improvement over $f = 0$, for all quantities except T, where all the models give similar results. For T, Y_V and P, $f = -sign(\nabla^2\overline{\phi})$ can be replaced by $f = 1$ if the signed $\overline{\sigma} = \sqrt{\overline{\phi\phi}} - \sqrt{\overline{\overline{\phi}\,\overline{\phi}}}$ is used instead of the positive $\overline{\sigma} = \left|\sqrt{\overline{\phi\phi}} - \sqrt{\overline{\overline{\phi}\,\overline{\phi}}}\right|$ of Equation 45. An alternative expression for f uses a scale-similarity idea, i.e. $f = sign(\phi - \overline{\phi}) = sign(\overline{\phi} - \overline{\overline{\phi}})$. This gives similar results to using $f = -sign(\nabla^2\overline{\phi})$ for all six variables. An analysis of the correlation $R(\phi, \overline{\phi})$ of Equation 44 showed that $R = 1$ for T and P, $0.97 < R < 1$ for u_1, u_2 and u_3 and $0.7 < R < 1$ for Y_V. For u_1, u_2 and u_3, the greatest deviation from 1 was in the middle of the mixing layer. For Y_V, the greatest deviation was at the droplet-laden/droplet-free interface. However, even in this region, $R = 1$ led to the best prediction of Y_V at droplet locations compared to smaller values. Most importantly, $R = 1$ is the only value that provides the correct $\overline{\sigma} \simeq 0$ in the laminar freestream. Finally, we note that the error for the approximation of Equation 46 is determined by that of the velocity components, which have the largest error of about 1.5%.

Models for Subgrid Cross-terms

For LES in the gas-phase, models are required for the subgrid stresses $\tau_{ij} = \widetilde{u_i u_j} - \widetilde{u}_i\widetilde{u}_j$, heat fluxes $\theta_j = \widetilde{Tu_j} - \widetilde{T}\widetilde{u}_j$ and species fluxes $\eta_j = \widetilde{Y_V u_j} - \widetilde{Y_V}\widetilde{u}_j$. For the droplet part, models are required for the subgrid variances σ^2_{SGS}: $\widetilde{u_1 u_1} - \widetilde{u}_1\widetilde{u}_1$, $\widetilde{u_2 u_2} - \widetilde{u}_2\widetilde{u}_2$, $\widetilde{u_3 u_3} - \widetilde{u}_3\widetilde{u}_3$, $\widetilde{\overline{T}\overline{T}} - \widetilde{\overline{T}}\,\widetilde{\overline{T}}$, $\widetilde{Y_V Y_V} - \widetilde{Y_V}\widetilde{Y_V}$ and $\widetilde{\overline{P}\overline{P}} - \widetilde{\overline{P}}\,\widetilde{\overline{P}}$. Since these two sets of terms are of the same form, it seems reasonable and consistent to use the same type of model for both. We consider three models, Smagorinsky, Gradient, and Scale-Similarity [15].

Smagorinsky SGS Model

$$\tau_{ij} = -2C_R\Delta^2\sqrt{\widetilde{S}_{kl}\widetilde{S}_{kl}}\left(\widetilde{S}_{ij} - \frac{1}{3}\widetilde{S}_{kk}\delta_{ij}\right) \qquad (47)$$

$$\theta_j = -\frac{C_R\Delta^2}{\mathrm{Pr}_t}\sqrt{\widetilde{S}_{kl}\widetilde{S}_{kl}}\frac{\partial\widetilde{T}}{\partial x_j} \qquad (48)$$

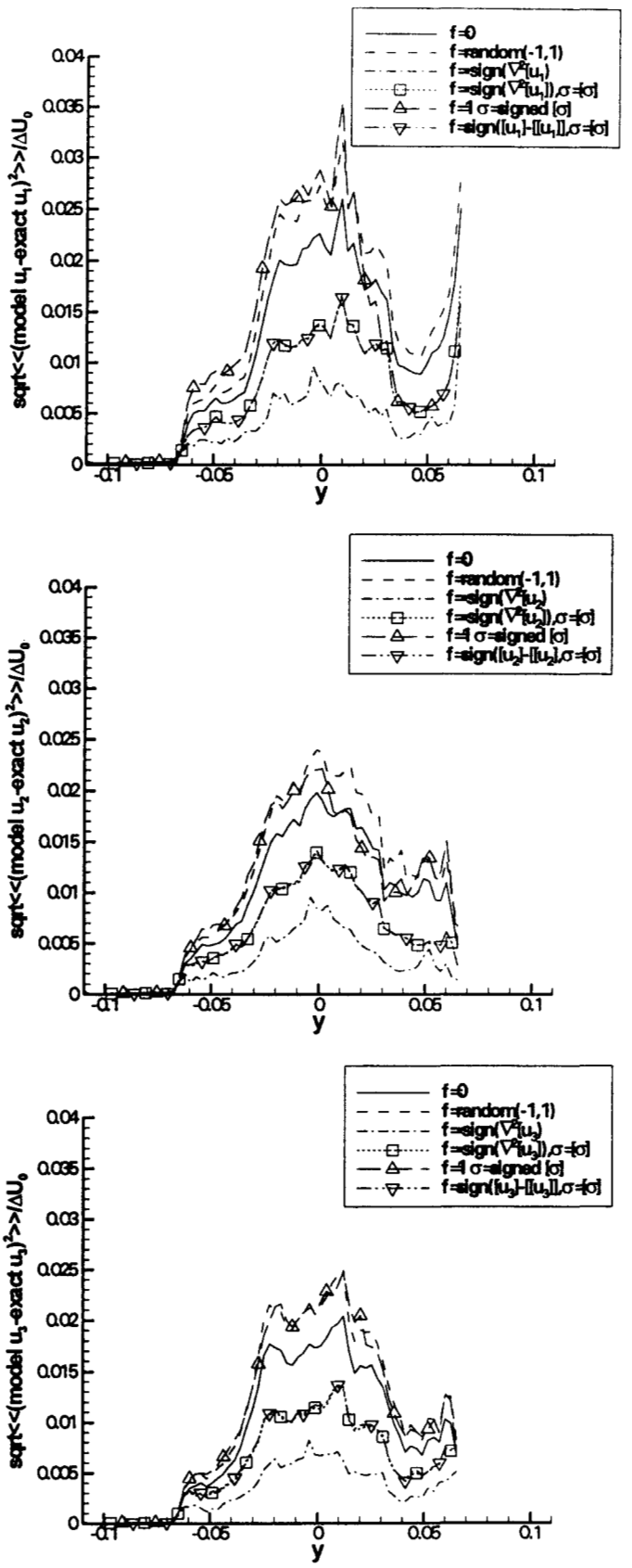

Figure 2: Error in unfiltered variable model $\phi = \overline{\phi} + f\sigma$ interpolated to droplet locations

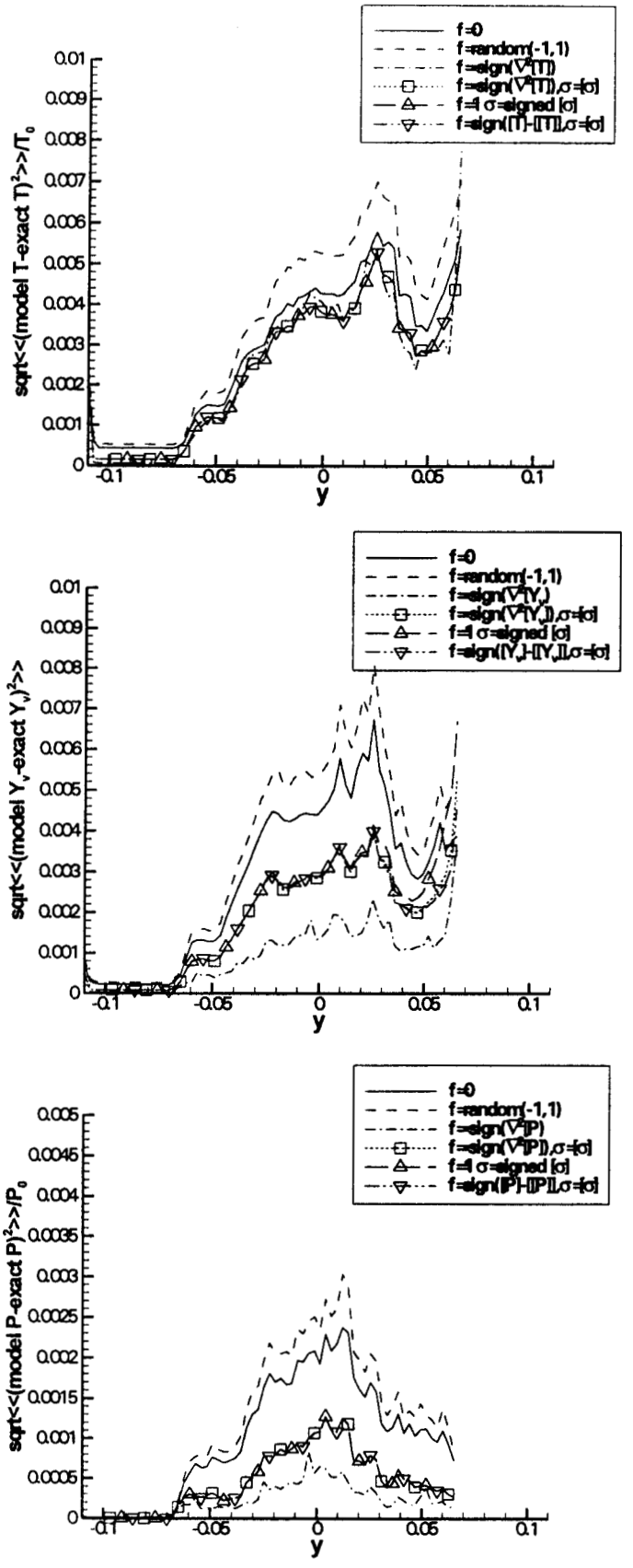

Figure 3: Error in unfiltered variable model $\phi = \overline{\phi} + f\sigma$ interpolated to droplet locations

$$\eta_j = -C_R \Delta^2 \sqrt{\widetilde{S}_{kl}\widetilde{S}_{kl}} \frac{\partial \widetilde{Y}_V}{\partial x_j} \tag{49}$$

with model constant C_R and filter width Δ, and where the rate-of-strain tensor is defined as

$$\widetilde{S}_{ij} = \frac{1}{2}\left(\frac{\partial \widetilde{u}_i}{\partial x_j} + \frac{\partial \widetilde{u}_j}{\partial x_i}\right) \tag{50}$$

Although this is forms the basis for most SGS modeling, it cannot be easily extended to compute the subgrid variances for T, P and Y_V.

Gradient SGS Model

$$\tau_{ij} = C_G \Delta^2 \frac{\partial \widetilde{u}_i}{\partial x_k}\frac{\partial \widetilde{u}_j}{\partial x_k} \tag{51}$$

$$\theta_j = C_G \Delta^2 \frac{\partial \overline{T}}{\partial x_k}\frac{\partial \widetilde{u}_j}{\partial x_k} \tag{52}$$

$$\eta_j = C_G \Delta^2 \frac{\partial \widetilde{Y}_V}{\partial x_k}\frac{\partial \widetilde{u}_j}{\partial x_k} \tag{53}$$

This model is easily extended to compute the subgrid variances for any quantity ϕ as

$$\sigma^2_{SGS}(\phi) = \overline{\phi\phi} - \overline{\phi}\,\overline{\phi} = C_G \Delta^2 \frac{\partial \overline{\phi}}{\partial x_k}\frac{\partial \overline{\phi}}{\partial x_k} \tag{54}$$

Theoretically, $C_G\Delta^2$ is the moment of the filtering volume, $I_c\Delta^2$ of Equation 40, as can be seen by integrating the square of the Taylor expansion for ϕ, Equation 38, over the filtering volume, but using filtered quantities in the derivatives. Thus for a cubic top-hat filter $C_G = \frac{1}{12}$. This model has the advantage that the derivatives are already available from the computation of the resolved part.

Scale-Similarity SGS Model

This model involves refiltering the flow-field at a test filter $\widehat{\Delta} \geq \Delta$

$$\tau_{ij} = C_S\left(\widehat{\widetilde{u}_i\widetilde{u}_j} - \widehat{\widetilde{u}}_i\widehat{\widetilde{u}}_j\right) \tag{55}$$

$$\theta_j = C_S\left(\widehat{\widetilde{u}_j\overline{T}} - \widehat{\widetilde{u}}_j\widehat{\overline{T}}\right) \tag{56}$$

$$\eta_j = C_S\left(\widehat{\widetilde{u}_j\widetilde{Y}_V} - \widehat{\widetilde{u}}_j\widehat{\widetilde{Y}}_V\right) \tag{57}$$

Theoretically, C_S should be 1. This model is easily extended to compute the subgrid variances for any quantity ϕ as

$$\sigma^2_{SGS}(\phi) = \overline{\phi\phi} - \overline{\phi}\,\overline{\phi} = C_S\left(\widehat{\phi\phi} - \widehat{\overline{\phi}}\,\widehat{\overline{\phi}}\right) \tag{58}$$

Model Coefficients

The validation of the models involves comparing the values predicted by the models to those obtained from the DNS database. Standard deviations from Equation 42 will be referred to as "exact". First, the correlation between the "exact" and model standard deviations will be computed.

Variable	Slope=$\sqrt{C_G}$	Correlation
u_1	0.4037	0.9855
u_2	0.4087	0.9847
u_3	0.4112	0.9835
T	0.3886	0.8727
Y_V	0.4155	0.9806
P	0.3980	0.9902
Combined	0.40	

Table 1: Gradient SGS Model $\Delta = 4\Delta x$

The correlations are computed by averaging over homogeneous $(x_1 - x_3)$ planes

$$R(X, Y; x_2) = \frac{< XY >}{\sqrt{< X^2 >}\sqrt{< Y^2 >}} \tag{59}$$

or over the whole domain

$$R(X, Y) = \frac{[XY]}{\sqrt{[X^2][Y^2]}} \tag{60}$$

By definition R is between -1 and 1. Values near 1 indicate strong positive correlation, values near -1 indicate strong negative correlation, whereas values near 0 indicate poor correlation. This allows pointwise assessment of the correlations. Next, the relationship between the two variables (i.e. the model coefficient) needs to be determined. The simplest is a constant-coefficient model where C_R, C_G, C_S are the same for all flow variables over the whole (spatial, temporal) domain. In that case, the coefficient can be determined using a least-squares fit to $Y = bX$ which leads to $b = [XY]/[XX]$. If X is the model standard deviation and Y is the "exact" standard deviation , then b is the square root of the model coefficient. More sophisticated models would have the model coefficients as functions of space and time.

Results

All three models were evaluated for Reynolds number of 600 and mass loading 0.2 (case TP600 of Miller and Bellan [9]) at the end of the simulation, using cubic top-hat filters.

Figure 4 shows the subgrid scale stresses predicted by the Smagorinsky model. It can be seen that there is little local correlation between the exact and predicted stresses. Thus, this model was not assessed further.

Figures 5 and 6 show the plane-averaged SGS standard deviations for u_1, u_2, u_3 and T, Y_V, P respectively. Deviations from both models show good correlations with the exact deviations, although the models tend to underpredict the temperature deviations. For these figures, values of $C_G = 0.4^2$ and $C_S = 0.79^2$ were used. These values were obtained from linear fits of the SGS standard deviations, which produced the coefficients presented in Tables 1 and 2.

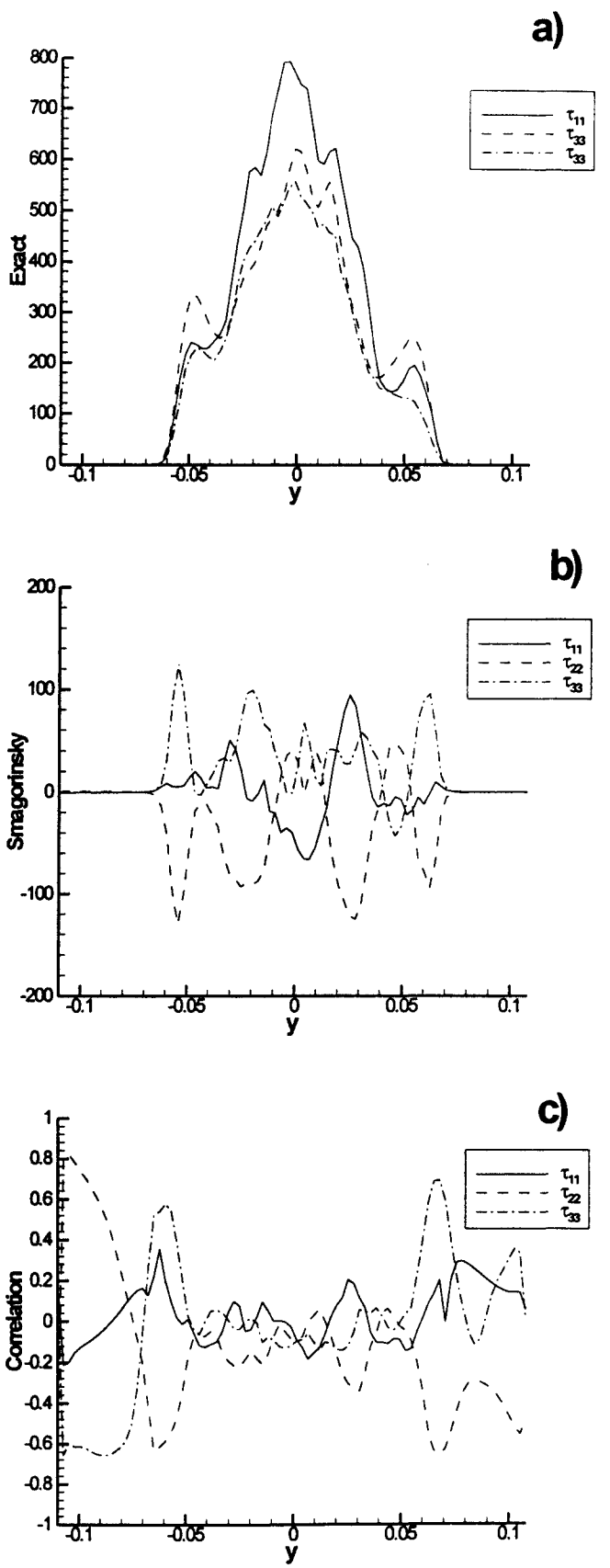

Figure 4: Subgrid stresses a)exact b)Smagorinsky c) correlation

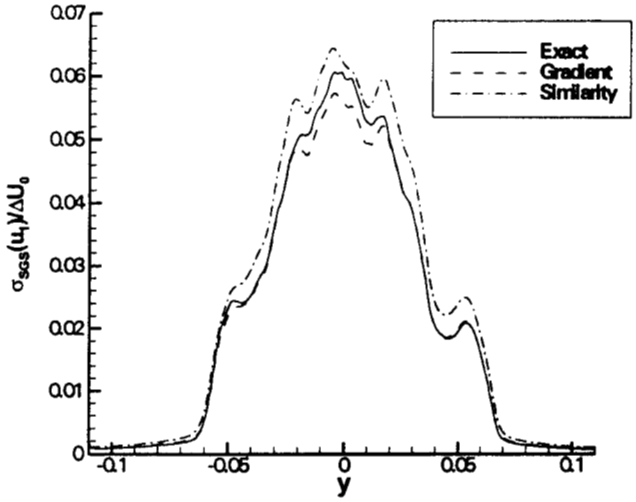

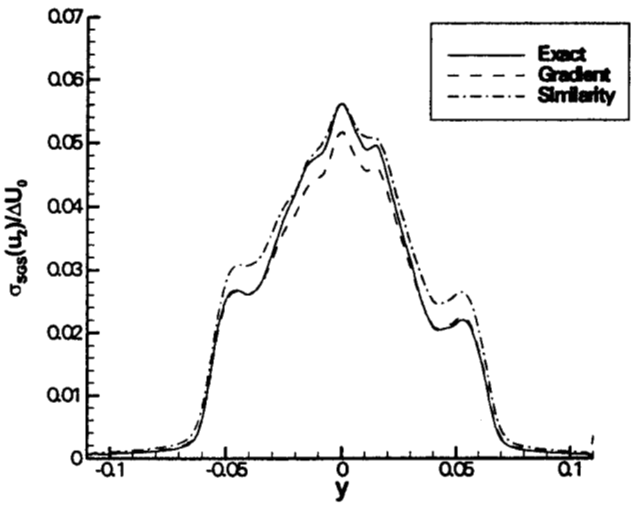

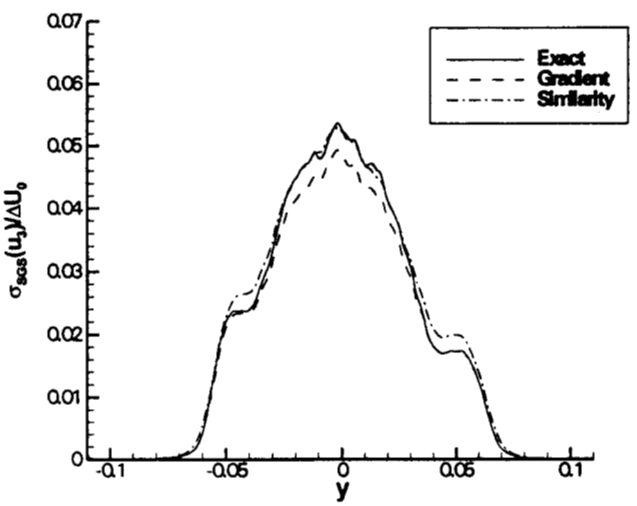

Figure 5: Plane Averages of SGS Standard Deviations, Velocity Components

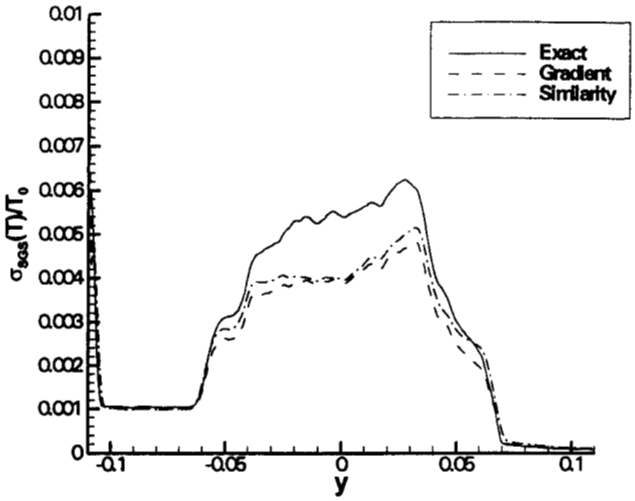

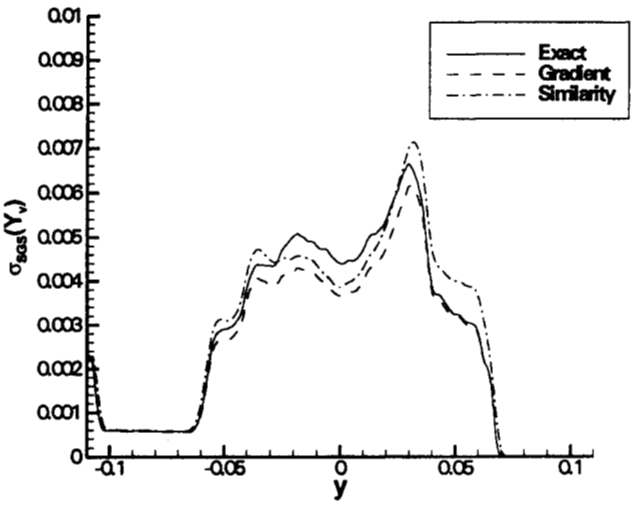

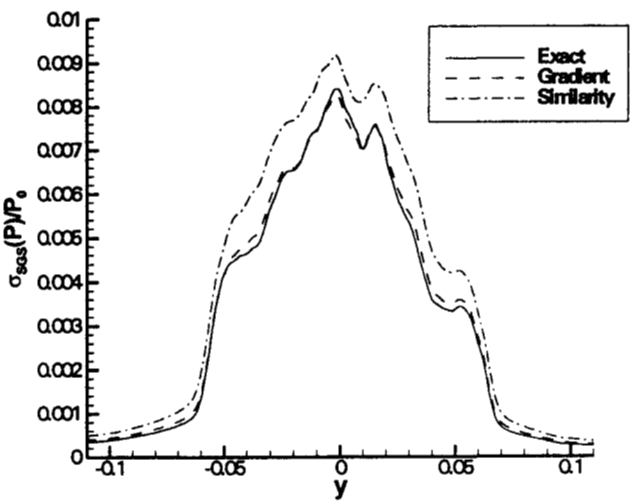

Figure 6: Plane Averages of SGS Standard Deviations, Temperature, Vapor Mass Fraction, and Pressure

Variable	Slope=$\sqrt{C_S}$	Correlation
u_1	0.7465	0.9475
u_2	0.7772	0.9498
u_3	0.8008	0.9498
T	0.9143	0.8958
Y_V	0.7856	0.9181
P	0.7350	0.9476
Combined	0.79	

Table 2: Scale-Similarity Model $\Delta = 4\Delta x; \widehat{\Delta} = 8\Delta x$

Conclusions

An a priori subgrid analysis has been conducted for a temporally developing mixing layer with evaporating droplets. This analysis was performed on a DNS database for Reynolds number (based on vorticity thickness) of 600 and mass loading of 0.2. Two models for the subgrid scale (SGS) standard deviations, the gradient and scale similarity models, where found to give excellent results when the model constant was properly calibrated. A model to recover the unfiltered variables from the filtered variables was also examined. In this model, the unfiltered variables are taken to be filtered variables plus a correction term which can be computed from the SGS standard deviations. Predictions for the unfiltered variables at the droplet locations were found to be improved compared to simply interpolating the filtered variables. Future work involves both testing these models on a DNS database for a higher mass loading and a posteriori testing of these models in an LES.

Acknowledgments

This research was conducted at the Jet Propulsion Laboratory (JPL) of the California Institute of Technology (Caltech). Computations were performed using the Caltech Center for Advanced Computing Research (CACR) parallel HP Exemplar.

References

[1] A. Ansari and W.Z. Strang. Large-Eddy Simulation of Turbulent Mixing Layers. Technical Report 96-0684, AIAA, 1996.

[2] M. Boivin, O. Simonin, and K.D. Squires. Direct Numerical Simulation of Turbulence Modulation by Particles in Isotropic Turbulence. *Journal of Fluid Mechanics*, 375:235–263, 1998.

[3] C.T. Crowe, T.R. Troutt, and J.N. Chung. Numerical Models for Two-Phase Turbulent Flows. *Annual Review of Fluid Mechanics*, 28:11–43, 1996.

[4] E. Deutsch and O. Simonin. Large Eddy Simulation Applied to the Modelling of Particulate Transport Coefficients in Turbulent Two-Phase Flows. In *Eighth Symposium on Turbulent Shear Flows*, pages 10–1:1–6, September 1991.

[5] S. Elghobashi and G.C. Truesdell. On the Two-Way Interaction Between Homogeneous Turbulence and Dispersed Solid Particles. I: Turbulence Modification. *Physics of Fluids A*, 5(7):1790–1801, 1993.

[6] F.F Grinstein and K. Kailasanath. Three-Dimensional Numerical Simulations of Unsteady Reactive Square Jets. *Combustion and Flame*, 100:2–10, 1995.

[7] D. Hansell, I.M. Kennedy, and W. Kollmann. A Simulation of Particle Dispersion in a Turbulent Jet. *International Journal of Multiphase Flow*, 18(4):559–576, 1992.

[8] F. Mashaayek. Droplet-Turbulence Interactions in Low-Mach-Number Homogeneous Shear Two-Phase Flows. *Journal of Fluid Mechanics*, 367:163–203, 1998.

[9] R.S. Miller and J. Bellan. Direct Numerical Simulation and Subgrid Analysis of a Transitional Droplet Laden Mixing Layer. Submitted to Physics of Fluids, 1999.

[10] R.S. Miller and J. Bellan. Direct Numerical Simulation of a Confined Three-Dimensional Gas Mixing Layer with One Evaporating Hydrocarbon-Droplet Laden Stream. *Journal of Fluid Mechanics*, 384:293–338, 1999.

[11] O. Simonin, E. Deutsch, and M. Boivin. Large Eddy Simulation and Second-Moment Closure of Particle Fluctuating Motion in Two-Phase Turbulent Shear Flows. *Turbulent Shear Flows*, 9:85–115, 1993.

[12] K.D. Squires and J.K. Eaton. Particle Response and Turbulence Modification in Isotropic Turbulence. *Physics of Fluids A*, 2(7):1191–1203, 1990.

[13] G.C. Truesdell and S. Elghobashi. On the Two-Way Interaction Between Homogeneous Turbulence and Dispersed Solid Particles. II. Particle Dispersion. *Physics of Fluids A*, 6(3):1405–1407, 1994.

[14] B. Vreman, B. Geurts, and H. Kuerten. A Priori Tests of Large Eddy Simulation of the Compressible Plane Mixing Layer. *Journal of Engineering Mathematics*, 29:299–327, 1995.

[15] B. Vreman, B. Geurts, and H. Kuerten. Large-Eddy Simulation of the Turbulent Mixing Layer. *Journal of Fluid Mechanics*, 339:357–390, 1997.

[16] Q. Wang, K.D. Squires, and O. Simonin. Large Eddy Simulation of Turbulent Gas-Solid Flows in a Vertical Channel and Evaluation of Second-Order Models. *International Journal of Heat and Fluid Flow*, 19:505–511, 1998.